35 p.

UNPUBLISHED PRELIMINARY DATA

GEOPHYSICS CORPORATION OF AMERICA BEDFORD, MASSACHUSETTS

National Aeronautics and Space Administration
Washington 25, D.C.

Covering the period 6 July thru 5 October 1963

GEOPHYSICS CORPORATION OF AMERICA
Bedford, Massachusetts

A STUDY OF THE METEOROLOGY OF MARS AND VENUS

Quarterly Progress Report No. 3

Contract No. NASw-704

TABLE OF CONTENTS

I. INTRODUCTION

During the past quarter, several topics of importance to the meteorology of Mars and Venus were under active study. The subject of atmospheric tides in the Martian atmosphere received a thorough treatment because of its possible importance to atmospheric circulations on the planet. Techniques for constructing thermodynamic diagrams for the Martian atmosphere were developed, and actual diagrams are under construction. These diagrams are useful in plotting temperature profiles, in analyzing convective processes, in studying water vapor condensation, and in studying other thermodynamic processes.

Research on the meteorology of Venus focused on two problems, both of them related to planetary and atmospheric temperatures. The first of these was an estimate of the amount of solar radiation absorbed by carbon dioxide in the atmosphere of Venus. Such a computation is of importance to greenhouse models, in which it is usually assumed that there is negligible absorption of the incoming solar radiation. The second problem concerned the temperature variation with altitude in the atmospheric layer between the planet's surface and the base of the cloud layer. Techniques for computing the radiative equilibrium distribution of temperature in this layer were developed.

Further discussions of these topics are presented in the following sections.

II. METEOROLOGY OF MARS

A. TIDES IN THE ATMOSPHERES OF EARTH AND MARS

A technical report entitled Tides in the Atmospheres of Earth and Mars by Richard A. Craig has been prepared and is in the process of publication. Professor Craig performed this study during the summer of 1963, when he was a visiting research scientist on the Meteorology of Mars and Venus project. The purpose and results of this study are summarized below.

Atmospheric tides — the atmospheric oscillations whose periods are equal to or sub-multiples of the solar or lunar day — is a subject of great interest to atmospheric scientists. One reason for this interest in the relatively small oscillations involved is the rather surprising observation that in our own atmosphere the solar semi-diurnal tide predominates over the lunar tide, which has a stronger gravitational excitation, and the solar diurnal tide, which has a stronger thermal excitation. Although all the details of this phenomenon are not clearly understood, it now appears that the predominance of solar tides over lunar is due to the importance of thermal excitation; and the relative strength of the solar semi-diurnal oscillation is due to a peculiar response of our atmosphere to the periodic heating.

The planet Mars is one for which application of tidal theory appears to have some interest. The relatively large diurnal temperature variation that is inferred for the surface of Mars raises the question of

the response thereto of the Martian atmosphere. The purpose of this study is to investigate this problem with the aid of standard tidal theory.

In the study of tidal oscillations, one first specifies a period which is equal to or a sub-multiple of the solar day (in our atmosphere one is also interested in periods similarly related to the lunar day, but this has no application to Mars). For the specified periods and a specified wave number, Laplace's tidal equation has a series of solutions in the form of Hough's functions, with each of which is associated a particular value of h, called an equivalent depth. Each of these solutions is spoken of as a mode of oscillation and describes the latitudinal behavior of the oscillation. Because the ratio of the length of the solar day to the length of the sideral day is essentially the same on Mars as on Earth, a given mode of oscillation has essentially the same form in the two atmospheres. On the other hand, the equivalent depth corresponding to a given mode of oscillation is less on Mars than on Earth because of differences in radius and mass of the planets.

In the case of free oscillations (not gravitationally or thermally forced), the radial equation is soluble for only one or two values of h, which are spoken of as eigenvalues. The number and magnitude of the eigenvalue(s) depend on the average vertical temperature distribution. The earth's atmosphere has only one such eigenvalue with a value of about 10 km. The earth's atmosphere would have a second eigenvalue of about 8 km if the

temperature near the stratopause were as high as was once thought likely. The temperature distribution in the Martian atmosphere is not well known. The temperature is believed to decrease upward, more rapidly near the surface than at higher levels. For a model atmosphere embodying these features, the Martian atmosphere also has one eigenvalue of about 20 km. This value does not depend very critically on the exact temperatures that are assumed. A second eigenvalue might arise if the temperature distribution at still higher levels were of a rather special character, but this possibility has not been explored.

The importance of the eigenvalues in tidal theory is as follows: if an excited mode of oscillation happens to have an equivalent depth whose value is very close to one of the eigenvalues, then that mode will be greatly amplified by resonance effects. A comparison of the equivalent depths on Mars for modes that might be excited by solar heating with the eigenvalue inferred for the Martian atmosphere indicates that no resonance magnification is to be expected.

Tidal oscillations on Mars might arise from the rather large diurnal temperature variation near the surface that is inferred from theory and observation. This possibility has been considered, and it appears highly improbable that the amplitude of the resulting diurnal surface-pressure oscillation (relative to the total surface pressure) exceeds the amplitude of earth's semi-diurnal oscillation. If this conclusion is correct, tidal oscillations arising from this cause are not likely to play any significant role in the Martian general circulation.

Tidal oscillations might also arise from diurnal or semi-diurnal temperature oscillations caused by periodic radiative processes occurring through deep layers of the Martian atmosphere. In our present state of knowledge about the composition of the Martian atmosphere, one cannot be sure about the amplitude of such temperature oscillations, but they are probably too small to excite significant tidal motions. If the atmosphere should contain ozone in amounts greater than now suspected (or any other gas that absorbs significant amounts of solar radiation), than this tentative conclusion would have to be re-examined.

Thus, in the context of present inferences about temperature and composition of the Martian atmosphere, there is no reason to expect that tidal motions play an important role in the meteorology of Mars.

B. THERMODYNAMIC DIAGRAMS FOR THE MARTIAN ATMOSPHERE

Diagrams for thermodynamic analyses of an atmosphere take into account water in its different phases. While diagrams for the earth's atmosphere are used for both research and weather forecasts, newly prepared diagrams for Mars would be used primarily for analyses of theoretical model atmospheres.

The parameters for isopleths on the Mars diagrams were chosen to be almost the same as the earth diagram (see enclosed diagram) parameters, which are pressure and approximate height, temperature, mixing ratio at water saturation, potential temperature, and wet-bulb potential

temperature or equivalent potential temperature. For a given vertical distribution of pressure, temperature, and relative humidity, a great deal of information can be obtained with the aid of five sets of lines of the earth's adiabatic charts. For each point of the distribution, the following quantities can be found: black-body radiation, saturation vapor pressure, actual vapor pressure, mixing ratio or specific humidity, dew point, pressure and temperature at the lifting condensation level, wet-bulb temperature, equivalent temperature, and approximate height above sea level. An analysis of the entire sounding can yield the following elements: thermal stability indices, distribution and amounts of positive and negative energy available for convection or work to be done by convection, pressures and temperatures at the level of free convection and at the convection condensation level, convection temperature, air mass identification, pressures and temperatures at a front aloft and at the tropopause, and approximate vertical thicknesses of layers. (Most of these elements are defined in meteorology textbooks, such as Holmboe, Forsythe, and Gustin, 1945.)

For the construction of thermodynamic diagrams for Mars, it was necessary to have the composition of the Martian atmosphere. "Dry air" on Mars was assumed to consist of 98% nitrogen and 2% carbon dioxide by volume. Water vapor was the only other constituent assumed. Although traces of other gases undoubtedly exist and may be important in radiation studies, they were considered as having a negligible influence on the specific gas constant averaged for the gaseous mixture. The mean surface

pressure was assumed to be 85 millibars in some diagrams and 20 millibars in another diagram (suggested by recent measurements). The following discussion considers what parameters are chosen and how they are represented.

The ordinate of a diagram should represent a scale of approximate height above the surface. The hypsometric formula suggests the choice of $- \log \left(\frac{p}{p_o}\right)$

$$z = - \frac{R}{g} T_m \ell n \left(\frac{p}{p_o}\right) \qquad (1)$$

where z is the height above the surface, R is the specific gas constant, g is the acceleration of gravity, T_m is the mean virtual temperature of the layer between p, the pressure, and p_o, the reference surface pressure. Since clouds, perhaps of water or ice, have been observed at a height of about 30 km, where $\frac{p}{p_o}$ is approximately 0.1, the ordinate should extend through at least one and preferably two logarithm cycles to the base 10. Diagrams with pressure ranges from 100 mb to 10 mb and from 20 mb to 0.2 mb were constructed.

The abscissa of a diagram should be a temperature function, the choice of which depends on the chief purpose of the diagram. For an area on the diagram to accurately represent energy or work, define the abscissa as T, the absolute temperature, and use semi-log paper. To have dry adiabats represented by straight lines, choose log T as the abscissa and use log-log paper. For radiation studies define the abscissa as log E and use log-log paper.

$$E = \sigma T^4, \tag{2}$$

where E is the blackbody radiation and σ is the Stefan-Boltzmann constant. Since

$$\log E = \log \sigma \text{ and } 4 \log T,$$

log E is linear in log T and also gives straight dry adiabats. If E is chosen to extend from .01 to 1 cal $cm^{-2}min^{-1}$ through two log cycles, the corresponding range of T from 105.3°K to 330.0°K is satisfactory for the Martian atmosphere.

The first set of lines to be drawn on the diagram is needed to represent the amount of water vapor for saturation with respect to water. Due to the low pressure on Mars, the specific humidity and mixing ratio may be significantly different at the higher temperatures (whereas they are assumed equal for the earth). For the purpose of deriving saturated adiabats later, q_{ws}, the saturation specific humidity, was chosen for Mars (instead of the saturation mixing ratio plotted on earth diagrams) because it gives the water vapor in terms of the total gas to be heated by condensation. For a given value of q_{ws}, T was tabulated (List, 1958, Table 94) from e_{ws}, the saturation vapor pressure, computed by Equation (4) and plotted against p.

$$e_{ws} = \frac{q_{ws}\, p}{f_w[\epsilon + (1 - \epsilon)\, q_{ws}]} \tag{4}$$

where f_w is a correction factor for the departure of water vapor from the ideal gas laws (List, 1958, Table 89) and

$$\epsilon = \frac{m_v}{m_d} = 0.635 \ , \tag{5}$$

the ratio of the molecular weight of water vapor to that of "dry air" on Mars. This ratio is 2% greater than 0.622, the value for the earth, due to a difference in m_d. Lines of constant q_{ws} were plotted for temperatures down to -50°C to allow for the supercooling of liquid water. These lines give the dew point changes with adiabatic pressure changes. Values of q_{ws} isopleths ranged from 0.5 g/kg to 1000 g/kg (= 1), the latter representing an atmosphere of pure water vapor and hence giving a line of T versus e_{ws} (read on the p scale). For any higher values of T, no saturation can occur, since

$$e \leq p < e_{ws}, \text{ or } \frac{e}{e_{ws}} < 100\% \tag{6}$$

where e is the actual vapor pressure (case of T above the boiling point).

The second set of lines for the diagram represents q_{is}, the saturation specific humidity with respect to ice. The low temperatures in the Martian atmosphere suggest the need for ice saturation data, which are not included on earth diagrams. The isopleths were drawn for the temperature range, -100°C up to 0°C, since the degree of supercooling of water is unknown and might be slight. The values range all the way from .001 g/kg to 1000 g/kg, the latter giving T versus e_{is}, the ice saturation

vapor pressure.

$$q_{is} < q_{ws} \text{ for } T < 0^{o}C \text{ and } q_{is} = q_{ws} \text{ at } T = 0^{o}C. \tag{7}$$

The q_{is} lines were prepared in the same way as the q_{ws} lines:

$$e_{is} = \frac{q_{is}\, p}{f_i[\epsilon + (1 - \epsilon)\, q_{is}]} \quad , \tag{8}$$

where the subscripts i refer to ice instead of liquid water. Tables were used as before (List, 1958, Tables 96 and 90). The q_{is} lines give the frost point in terms of pressure for dry adiabatic processes.

The next set of lines represents the dry adiabats, which give the relation between T and p for adiabatic processes without condensation or evaporation, namely at constant θ, potential temperature:

$$\frac{T}{\theta} = \left(\frac{p}{p_o}\right)^{K} , \quad K = \frac{R}{C_p} \tag{9}$$

where R is the specific gas constant for the atmospheric mixture and C_p is the specific heat at constant pressure. K = 0.285, the same for Mars as for the earth.

$$\log T = \log \theta + K \log \left(\frac{p}{p_o}\right) . \tag{10}$$

On log-log paper, the adiabats have a constant slope of $\frac{1}{K}$, which makes them parallel as well as straight lines. Since θ is defined as the

temperature of air reduced dry adiabatically from p to p_o, θ on the Mars diagram is the same as θ on the earth diagram only if p_o is 1000 mb. Hence, the dry adiabats on the earth's diagram can be used without any changes for the Martian atmosphere. However, for Mars with its low pressure, a lower value of p_o might be more appropriate. If p_o is chosen as 100 mb, the newly defined θ values will be the same as the θ values on the earth diagram provided that its pressure labels on the ordinate scale are all divided by 10. Another choice of p_o is to make θ of Mars equal to half of θ of the earth. This requires

$$\left(\frac{p_o}{1000\ \text{mb}}\right)^K = \frac{1}{2}\ , \quad \text{or } p_o = 87.7\ \text{mb}\ . \tag{11}$$

Again, the earth adiabatic chart can be used, but this time θ values are divided by 2 instead of p values divided by 10. Regardless of what different p_o values are used for Mars, the dry adiabats and their labels are not affected as long as the ordinate scale is labeled p/p_o and if p_o is the reference pressure for the definition of θ. The construction of dry adiabats on semi-log paper is difficult because they are not straight lines. One way to accomplish this is to read p and T from selected points along a straight adiabat on a diagram presented on log-log paper or on a Stüve diagram, of $-\left(\frac{p}{p_o}\right)^K$ versus T, then plot these points on semi-log paper and connect them with a smooth curve.

The final set of lines represents the saturation adiabats (curves of constant θ_{ws}, saturation wet-bulb potential temperature, or curves of

constant θ_{es}, saturation equivalent potential temperature) showing the temperature changes when adiabatic pressure changes cause condensation or evaporation, with the release or consumption of L_w, the latent heat of vaporization, reducing the dry adiabatic temperature changes. The saturation adiabats can be constructed from the approximation formula,

$$(dT)_p = - \frac{L_w}{C_p} \, dq_{ws} \quad , \tag{12}$$

where $(dT)_p$ is the isobaric temperature increase resulting from a decrease of $-dq_{ws}$ in saturation specific humidity resulting from condensation. For a temperature of 220^oK, $\frac{L_w}{C_p}$ on Mars is $-2.57 \times 10^3 \, dq_{ws} \, C^o$, which is roughly the value, $-2.5 \times 10^3 \, dq_{ws} \, C^o$, used for the earth (Holmboe, Forsythe, and Gustin, 1945, p.73). A method of constructing the saturation adiabats is to draw diagonals across imaginary approximate parallelograms formed by θ and q_{ws} lines at intervals of 5 C^o and 2g/kg, respectively. The diagonals must be drawn so that the changes in θ and q_{ws} are in the opposite sense along them. To be correctly drawn, the slope of each saturation adiabat must be intermediate between the slopes of the saturation specific humidity lines and of the dry adiabats. The increase in θ with condensation is assumed to be equal to the increase in T. This is true at $p = p_o$, but the increase of θ should be 22% (or 1 C^o) larger at $p = \frac{1}{2} p_o$ to get the same increase of T. This error was ignored in the construction of the saturated adiabats because they were drawn only for $p_o \geq p \geq \frac{1}{2} p_o$. They were not carried any higher because they diverged upward toward lower pressure, thereby becoming more inaccurate. Curves were drawn for equally spaced value of θ_{ws} (rather than

θ_{es}), defined as the temperature of saturated air reduced by a saturated adiabatic process to the pressure p_o (instead of 1000 mb as defined for the earth). Although the saturation adiabats were constructed for condensation into water, they could have been drawn for sublimation into ice, using L_i, the latent heat of sublimation. At 220°K, the constant $\frac{L_i}{C_p}$ on Mars is $-2.75 \times 10^3 \, dq_{is} \, C^o$. The sides of the approximate parallelograms used in construction would be $5\frac{1}{2}$ C^o and 2 g/kg for θ and q_{is}, respectively.

The four sets of lines for the Mars diagrams, described above, are quite similar to the lines on the earth diagrams. However, a big difference between the two planets appears when the height scale for Mars is compared with the earth's height scales because of the small gravity (376 cm/sec^2) on Mars. A model atmosphere was plotted on the diagrams for Mars, showing T versus p. The surface temperature was assumed to be 230°K. The lapse rate was assumed to be dry adiabatic up to a tropopause at a height of 20 km and to be isothermal in the Martian stratosphere. The dry adiabatic lapse rate for Mars is

$$\gamma_d = -\frac{dT}{dz} = \frac{g}{C_p} = 3.65 \ K^o/km \ , \qquad (13)$$

about 1/3 of that of the earth.

The temperature at $z \geq 20$ km in this model atmosphere is 157°K. At 20 km p/p_o is .263. For p_o = 85 mb or 20 mb, at 20 km p = 22 1/3 mb or 5 1/4 mb, respectively. The formulas used for computing the pressure

at chosen heights were

$$\left(\frac{p}{p_o}\right)^{2/7} = 1 - \frac{\gamma_d z}{T_o} = 1 - .01587\ z\ km^{-1} \quad \text{for } z \leq 20\ km, \tag{14}$$

where the subscript o refers to the surface of Mars, and

$$\frac{p}{p_{20}} = \exp\left[- \frac{\gamma_d (z - 20\ km)}{K\ T_{20}} \right] = \exp\left[-.08153\ km^{-1}\ (z - 20\ km) \right] \tag{15}$$

$$\text{for } z \geq 20\ km,$$

where the subscript 20 refers to the 20-km level.

The actual diagrams for Mars are in the process of construction and will be available in a forthcoming report.

III. METEOROLOGY OF VENUS

A. ABSORPTION OF SOLAR RADIATION BY CARBON DIOXIDE IN THE VENUS ATMOSPHERE

In greenhouse models of the Venus atmosphere, it is generally implicitly assumed that the portion of the solar radiation that is not reflected back to space reaches the surface of the planet. Actually, however, some of the radiation is probably absorbed in the very thick atmosphere of the planet, and in the cloud layer. Since the composition of the cloud layer is unknown, it is difficult to estimate how much depletion of the solar beam takes place in the clouds. Estimates of direct absorption by the atmosphere are also difficult since the atmospheric composition is uncertain, carbon dioxide being the only gas definitely detected. In this section, we attempt to estimate the amount of solar radiation absorbed by the near-infrared bands of carbon dioxide in the Venus atmosphere.

Howard, Burch and Williams (1956) have presented empirical relations relating absorption to path length and pressure for several CO_2 bands. For weak absorption by a minor atmospheric constituent, the empirical equations are of the form

$$A = \int_{\nu_1}^{\nu_2} A_\nu \, d_\nu = c \left[up^{2k} \right]^{\frac{1}{2}} \tag{16}$$

where A is the band absorption, A_ν is the absorption at wavenumber ν, u is the absorber path length in cm NTP, and p is the atmospheric pressure in mm Hg. The values of the empirical constants c and k vary from

band to band. For strong absorption (where $\int_{\nu_1}^{\nu_2} A_\nu \, d\nu$ is greater than an empirical value that varies from band to band) they obtained

$$A = \int_{\nu_1}^{\nu_2} A_\nu \, d_\nu = C + D \log up^{K/D} \tag{17}$$

The empirical constants for the different bands of interest of this study are shown in Table I.

The column labelled "Determining A" provides the basis for using either the weak or strong fit.

A model atmosphere has been constructed for Venus by Kaplan (1963), and this can be used to obtain an estimate of the total CO_2 path length u. The path length can be determined from

$$u = \frac{m_c}{m_v} \frac{\int_o^\infty \rho_c \, dz}{\rho_c'} = \frac{m_c}{m_v} \left(\frac{1}{\rho_c'}\right) \left(\frac{\rho_c}{\rho_v}\right) \frac{1}{g} p_o \tag{18}$$

where m_c is the molecular weight of carbon dioxide, m_v is the molecular weight of the Venus atmosphere, ρ_c is the density of carbon dioxide, ρ_c' is the density of CO_2 at STP, (ρ_c/ρ_v) is the volume percentage of CO_2, g is gravity, and p_o is surface pressure. Using the values $m_c = 44$; $m_v = 29.6$; $\rho_c' = 1.94 \times 10^{-3}$ g cm^{-3}; $(\rho_c/\rho_v) = 0.10$; g = 900 cm sec^{-2}; and p_o = 10 atm = 10^7 dynes cm^{-2}, we obtain u = 1.1×10^6 cm STP.

TABLE I

EMPIRICAL RELATIONS FOR CO_2 BANDS

Band (μ)	Band Limits (cm^{-1})	Weak Fit C	K	Determining A (cm^{-1})
5.2	1870 - 1980	.024	.40	< 30
4.8	1980 - 2160	.12	.37	60
4.3	2160 - 2500	--	--	50
2.7	3480 - 3800	3.15	.43	50
2.0	4750 - 5200	.492	.39	80
1.6	6000 - 6550	.063	.38	80
1.4	6650 - 7250	.058	.41	80

Band (μ)	Band Limits (cm^{-1})	Strong Fit C	D	K
4.3	2160 - 2500	27.5	34	31.5
2.7	3480 - 3800	-137.0	77	68.0
2.0	4750 - 5200	-536.0	138	114.0

Examination of Equation (16) for the weak fit and the weak fit part of Table I reveals that, with this much carbon dioxide and with the pressures prevailing on Venus, the strong fit must be used for all the carbon dioxide bands. Unfortunately several of the bands do not have strong fit relations. However, King (1963) has developed a theoretical relationship some of the constants in the strong and weak fits and we can use this relationship to obtain an estimate of the necessary strong fits. King's relationship is

$$\log .8686\ D + \frac{C}{2D} = -\log c - .4343\delta \qquad (19)$$

where $\delta = 0.981$.

Thus, given D and C one can estimate c. However, we would like to obtain estimates of D and C, given c. In order to accomplish this we have assumed that there is an approximate relationship between D and C of the form $D = a + b\ C$. From Howard et al's values of D and C for CO_2 bands, we have determined, by a least squares procedure, the relationship

$$D = 43.9 - .180\ C \qquad (20)$$

By substituting this relation in (19) we now have a means of determining C (the strong fit constant) from c (the weak fit constant). This has been done for the 5.2μ, 4.8μ, 1.6μ, and 1.4μ bands, and these results as well as the Howard et al results for 4.3μ, 2.7μ, and 2.0μ are shown in Table II.

TABLE II

STRONG FIT RELATIONS FOR CO_2 BANDS

Band (μ)	Band Limits (cm^{-1})	C	D	K
5.2	1870 - 1980	-49.5	52.8	----
4.8	1980 - 2160	-243.0	87.6	----
4.3	2160 - 2500	27.5	34.0	31.5
2.7	3480 - 3800	-137.0	77.0	68.0
2.0	4750 - 5200	-536.0	138.0	114.0
1.6	6000 - 6550	-137.0	68.6	----
1.4	6650 - 7250	-127.0	66.0	----

The values for 4.3μ, 2.7μ, and 2.0μ indicate that the ratio K/D, needed for Equation (17), is about 0.9. We have therefore assumed that K/D is equal to 0.9, independent of band.

We can write Equation (17) in the following form

$$A = C + D \log u_r \tag{21}$$

where $u_r = up^{K/D}$ for a path at constant pressure, and $u_r = \int_{u(p_1)}^{u(p_2)} p^{K/D}\, du$ for a path through an atmosphere with varying pressure; for the atmosphere of Venus we must use the second relationship for u_r. Since the CO_2 mixing ratio is constant with altitude the CO_2 path length is directly proportional to pressure, and we have $u = \alpha p$, $du = \alpha dp$, and $u_o = \alpha p_o$, where u_o is the total CO_2 path length, and p_o is surrace pressure.

Then

$$u_r = \alpha \int_o^{Po} p^{K/D}\, dp \tag{22}$$

Integration of this expression yields

$$u_r = \frac{u_o\, p_o^{K/D}}{(K/D) + 1}$$

With $u_o = 1.1 \times 10^6$ cm STP, $p_o = 7.6 \times 10^3$ mm, and K/D = 0.9, the reduced path length u_r is equal to 9×10^8.

The absorption A can now be computed for each of the bands in Table II with the use of Equation (21). The fractional absorption of each

of these bands can be obtained from

$$a = \frac{A}{\Delta\nu}$$

where $\Delta\nu$ is the width of the band in cm^{-1}. The computed values of fractional absorption a are shown in Table III.

Since the real value of the fractional absorptivity cannot be greater than unity, all bands with computed values of a greater than one were assumed to have fractional absorptivities of unity.

In order to compute the absorption of solar radiation in the Venus atmosphere by these CO_2 bands, we must first determine the amount of solar energy available for absorption. This amount depends essentially upon Venus' distance from the Sun, and the planetary albedo at the different wavelengths. Table IV indicates the solar radiation intensities, albedos, available radiation intensities, absorptivities, and finally absorbed energy values for each of the CO_2 bands. The solar radiation intensities are based upon a $6000^{o}K$ blackbody Sun, a fair approximation in the near infrared. The albedos are after Sinton (1963). The last figure in the last column is the total amount of solar radiation absorbed in the Venus atmosphere by these CO_2 bands. Since the total solar insolation at the top of the atmosphere is about 2650 watts m^{-2}, the CO_2 absorption amounts to over 3% of this values. The integrated planetary albedo of Venus is about 0.73 (Sinton, 1962) so that, after correcting for albedo losses, the amount of energy remaining before absorption processes is about 715 watts m^{-2}. The CO_2 absorption, 83.2 watts m^{-2}, is about 12% of this value.

TABLE III

FRACTIONAL ABSORPTION BY CO_2 BANDS

Band (μ)	a(computed)	a(adopted)
5.2	3.8	1.0
4.8	3.0	1.0
4.3	0.98	0.98
2.7	1.7	1.0
2.0	1.56	1.0
1.6	0.87	0.87
1.4	0.79	0.79

TABLE IV

COMPUTATION OF CO_2 ABSORPTION IN VENUS ATMOSPHERE

Band (μ)	$\Delta\lambda$ ($m\mu$)	Intensity Outside Atmosphere I(watts m^{-2})	Albedo A	Available Energy (1 - A)I	Absorptivity a	CO_2 Absorption a(1 - A)I watts m^{-2}
5.2	5348-5051	1.9	.15	1.6	1.0	1.6
4.8	5051-4630	3.7	.15	3.1	1.0	3.1
4.3	4630-4000	8.5	.15	7.2	0.98	7.1
2.7	2874-2632	10.2	.15	8.7	1.0	8.7
2.0	2105-1923	37.4	.40	22.4	1.0	22.4
1.6	1667-1527	59.9	.52	28.8	0.87	25.1
1.4	1504-1379	76.7	.75	19.2	0.79	15.2
						83.2

We may conclude from these estimates that the assumption that all of the unreflected solar radiation reaches the surface of Venus is is error by at least 12%, since CO_2 alone is capable of absorbing this amount. Absorption by the clouds and other atmospheric constituents would increase this figure.

B. RADIATIVE EQUILIBRIUM DISTRIBUTION OF TEMPERATURE BELOW THE VENUS CLOUD LAYER

Observational evidence indicates that the planet Venus is covered by an extensive cloud layer. It would be of interest to attempt a theoretical determination of the vertical variation of temperature between the surface of the planet and the base of the cloud layer. Estimates are available for the surface temperature and the cloud temperatures. If we assume that the atmosphere between the cloud base and surface is in infrared radiative equilibrium, we can compute a radiative equilibrium temperature distribution between these two levels. The computed temperature distribution may serve as a useful estimate of the actual temperature distribution, if the assumption and model used for the computations are not too unrealistic. In this section we develop a technique for making this kind of computation.

It is assumed that the cloud layer completely covers the sky and that both the cloud base and planetary surface radiate as blackbodies at fixed temperatures. It is further assumed that the atmospheric layer between the cloud base and planetary surface is a grey absorber and is in infrared radiative equilibrium. The net infrared flux at any opacity level τ within this atmospheric layer can then be written as

$$F(\tau) = 2B(o)E_3(\tau) - 2B(b)E_3(\tau_b - \tau) + 2\int_o^{\tau} B(t)E_2(\tau - t)dt - 2\int_{\tau}^{\tau_b} B(t)E_2(t - \tau)dt \tag{23}$$

where $\tau = \int_o^z k\rho dz$, k being the grey absorption coefficient, ρ the density of the absorbing gas, and z the height; B(o) is the blackbody radiation flux from the surface; B(b) is the blackbody radiation flux from the cloud base; B(t) is the blackbody flux at any level within the atmospheric; and E's are exponential integrals. The infrared opacity is taken as zero at the surface, increasing to τ_b at the cloud base (see sketch).

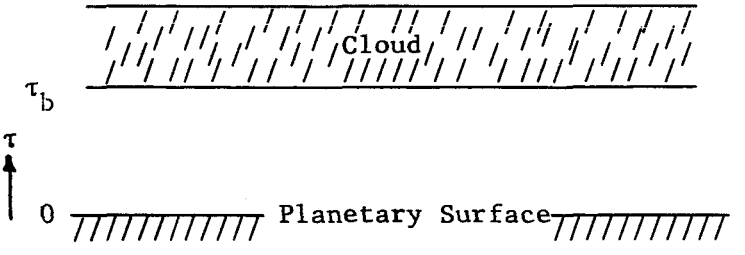

Under conditions of radiative equilibrium $\frac{dF}{d\tau} = 0$. Differentiating Equation (23) with respect to τ, one obtains

$$\frac{dF}{d\tau} = -B(b)E_2(\tau_b - \tau) - B(o)E_2(\tau) - \int_o^{\tau} B(t)E_1(\tau - t)dt - \int_o^{\tau_b} B(t)E_1(t - \tau)dt + 2\,B(\tau). \tag{24}$$

Setting this expression equal to zero and solving for $B(\tau)$, one obtains

$$B(\tau) = \frac{1}{2}\left[B(o)E_2(\tau) + B(b)E_2(\tau_b - \tau) + \int_o^{\tau_b} B(t)E_1(|\tau - t|)dt\right] \tag{25}$$

This equation can be written in terms of temperature with the use of relationship $B = \sigma T^4$; one then obtains

$$T^4(\tau) = \frac{1}{2}\left[T^4(o)E_2(\tau) + T^4(b)\ E_2(\tau_b - \tau) + \int_o^{\tau_b} T^4(t)E_1(|\tau - t|)dt\right] \qquad (26)$$

We would like to obtain $T(\tau)$ from this equation, given $T^4(o)$, $T^4(b)$, and τ_b. The following discussion indicates the numerical techniques used to obtain the required variation of temperature with τ.

The object of this work is to solve the second order integral equation,

$$T^4(\tau) = A(\tau) + \int_o^{\tau_b} \epsilon(\tau,t)T^4(t)dt \qquad (27)$$

where

$$A(\tau) = \frac{1}{2}\left[T^4(o)E_2(\tau) + T^4(\tau_b)E_2(\tau_b - \tau)\right]$$

and

$$\epsilon(\tau,t) = \frac{1}{2}\left[E_1(|\tau - t|)\right]$$

for $T(\tau)$, the temperature in degrees Kelvin, at the point, τ, and obtain a temperature distribution in the interval, $o \leq \tau \leq b$.

The usual procedure for solving this type of equation is to consider a discrete set of points $(\tau_1, \tau_2, \ldots\ldots \tau_n)$ in the interval, $o \leq \tau \leq \tau_b$, and to approximate the integral Equation (27) at each point τ_i, as the sum,

$$T^4(\tau_i) = A(\tau_i) + \sum_{j=1}^{n} \epsilon(\tau_i, \tau_j) T^4(\tau_j) D(\tau_j), \quad (i = 1, 2, \ldots, n) \tag{28}$$

where $D(\tau_j)$ is a function of the interval $\Delta\tau_j = \tau_{j+1} - \tau_j$, depending on the method used for approximating the integral of Equation (27).

This procedure reduces the problem to solving the following matrix equation,

$$\begin{pmatrix} T_1 \\ T_2 \\ \cdot \\ \cdot \\ \cdot \\ T_n \end{pmatrix} = \begin{pmatrix} A_1 \\ A_2 \\ \cdot \\ \cdot \\ \cdot \\ A_n \end{pmatrix} + \begin{pmatrix} \epsilon_{11}D_1 & \epsilon_{12}D_2 & \ldots\ldots & \epsilon_{1n}D_n \\ \epsilon_{21}D_1 & \epsilon_{22}D_2 & \ldots\ldots & \epsilon_{2n}D_n \\ \cdot & & & \\ \cdot & & & \\ \cdot & & & \\ \epsilon_{n1}D_1 & \epsilon_{n2}D_2 & \ldots\ldots & \epsilon_{nn}D_{nn} \end{pmatrix} \begin{pmatrix} T_1 \\ T_2 \\ \cdot \\ \cdot \\ \cdot \\ T_n \end{pmatrix} \tag{29}$$

where

$$A_i = A(\tau_i)$$

$$\epsilon_{ij} = \epsilon(\tau_i, \tau_j)$$

$$T_i = T^4(\tau_i)$$

Difficulty arises in evaluating Equation (29) for T_i, however, because the diagonal elements of the kernal are singular, i.e.

$$\epsilon_{ii} = \frac{1}{2} E_1(|\tau_i - \tau_i|) = \frac{1}{2} E_1(o) = \infty \tag{30}$$

In the problem at hand, this anomaly was eliminated by slightly modifying the above procedure. The method is outlined below.

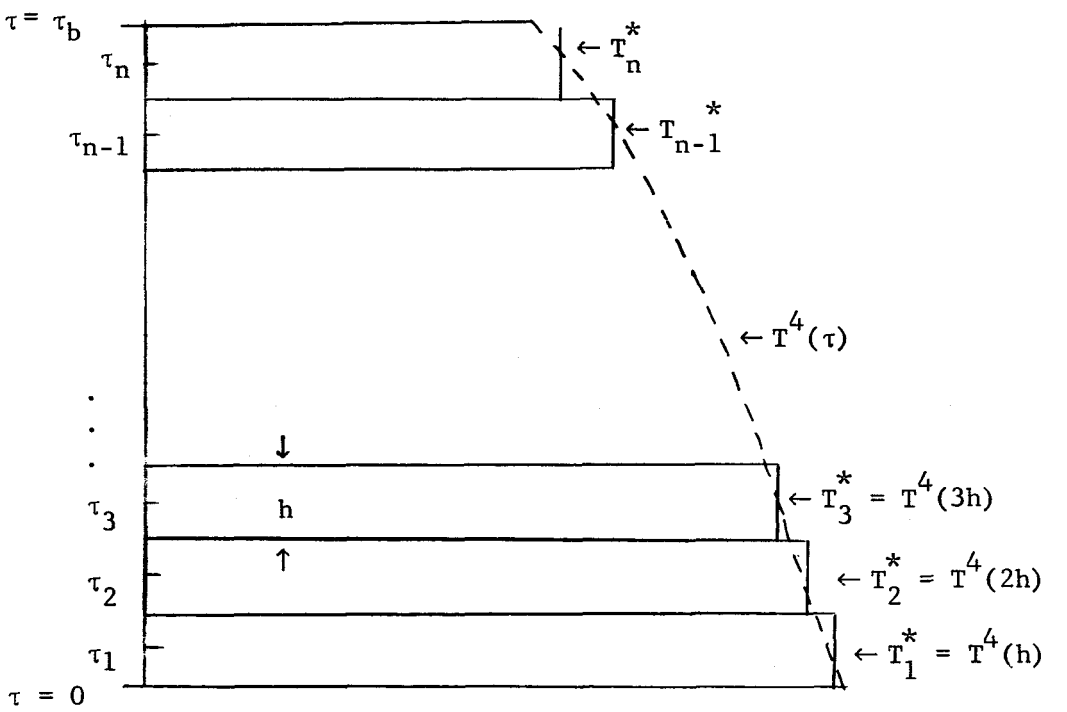

Instead of attempting to evaluate the temperature at certain points in the interval $0 \leq \tau \leq \tau_b$, the interval is divided into equal segments of length, h, (see sketch), and the temperature is considered constant in each segment. This assumption is justified since the function $T(\tau)$ is regular in the interval, and the segment, h, can be made small enough such that the change in temperature within any segment is negligible.

Thus, with $T(\tau)$ constant in each segment, the integral of Equation (27) can be directly integrated over each segment, and the matrix Equation (29) reduces to the following:

$$\begin{pmatrix} T_1^* \\ \cdot \\ \cdot \\ \cdot \\ T_n^* \end{pmatrix} = \begin{pmatrix} A_1^* \\ \cdot \\ \cdot \\ \cdot \\ A_n^* \end{pmatrix} + \begin{pmatrix} \frac{1}{2}\int_o^h E_1(|\tau_1 - t|)\,dt & \cdots\cdots & \frac{1}{2}\int_{(n-1)h}^{nh=\tau_b} E_1(t-\tau_1)\,dt \\ \cdot & & \cdot \\ \cdot & & \cdot \\ \cdot & & \cdot \\ \frac{1}{2}\int_o^h E_1(\tau_n - t)\,dt & \cdots\cdots & \frac{1}{2}\int_{(n-1)h}^{nh=\tau_b} E_1(|\tau_n - t|)\,dt \end{pmatrix} \begin{pmatrix} T_1^* \\ \cdot \\ \cdot \\ \cdot \\ T_n^* \end{pmatrix} \qquad (31)$$

where,

$$T_k^* = T^4(kh)$$

$$A_k^* = \frac{1}{2}\left\{T^4(o)E_2[(k - \tfrac{1}{2})h] + T^4(\tau_b)E_2[(n - k + \tfrac{1}{2})h]\right\}$$

Integrating the elements of the kernal matrix, and denoting them by K_{ij},

$$K_{ii} = \frac{1}{2}\int_{(i-1)h}^{ih} E_1(|\tau_i - t|)\,dt = \frac{1}{2}\int_{(i-1)h}^{(i-\frac{1}{2})h} E_1(\tau_i - t)\,dt + \frac{1}{2}\int_{(i-\frac{1}{2})h}^{ih} E_1(t-\tau_i)\,dt$$

$$= \tfrac{1}{2}\,E_2(o) - \tfrac{1}{2}\,E_2(\tfrac{1}{2}\,h) - \tfrac{1}{2}\,E_2\,(\tfrac{1}{2}\,h) + \tfrac{1}{2}\,E_2(o)$$

$$= 1 - E_2(h/2)$$

$$K_{ij} = \frac{1}{2}\int_{(j-1)h}^{jh} E_1(\tau_i - t)\,dt = \frac{1}{2}\left\{E_2[\tau_i - jh] - E_2[\tau_i - (j-1)h]\right\} \quad i > j$$

$$K_{ij} = \frac{1}{2} \int_{(j-1)h}^{jh} E_1(t-\tau_i)\,dt = \frac{1}{2} \left\{ E_2[(j-1)h - \tau_i] - E_2[jh - \tau_i] \right\} \quad i < j$$

The solution is,

$$\begin{pmatrix} T_1^* \\ T_2^* \\ \cdot \\ \cdot \\ \cdot \\ T_n^* \end{pmatrix} = \begin{pmatrix} 1-K_{11} & -K_{12} & \cdots & -K_{1n} \\ -K_{21} & 1-K_{22} & \cdots & -K_{2n} \\ \cdot & & & \cdot \\ \cdot & & & \cdot \\ \cdot & & & \cdot \\ -K_{n1} & -K_{n2} & & 1-K_{nn} \end{pmatrix}^{-1} \begin{pmatrix} A_1^* \\ A_2^* \\ \cdot \\ \cdot \\ \cdot \\ A_n^* \end{pmatrix} \tag{32}$$

A program has been constructed to evaluate Equation (32) for as many as fifteem segments, giving numerical values of T_i^* with seven place accuracy.

IV. FUTURE PLANS

It is planned to complete construction of the thermodynamic diagrams for the Martian atmosphere.

Work on an estimate of the radiation budget for Mars has begun and will be continued.

Computations of the radiative equilibrium temperature distribution between the cloud base and surface of Venus will be performed with the model discussed in this report.

REFERENCES

Holmboe, J., G.E. Forsythe, and W. Gustin, 1945: Dynamic Meteorology, New York, Wiley

Howard, J.N., D.E. Burch, and D. Williams, 1956: Infrared transmission of synthetic atmospheres II. Absorption by carbon dioxide. J. Opt. Soc. Amer., 46, 237-241.

King, J.I.F., 1963: Private communication.

List, R.J., 1958: Smithsonian Meteorological Tables, 6th Revised Edition, Washington, Smithsonian Institute.